SLAC-PUB-2453
January 1980
(T/E)

DYNAMICAL BREAKING OF CHIRAL SYMMETRY IN LATTICE GAUGE THEORIES*

Benjamin Svetitsky, Sidney D. Drell,
Helen R. Quinn, and Marvin Weinstein

Stanford Linear Accelerator Center
Stanford University, Stanford, California 94305

ABSTRACT

We generalize the variational block spin methods developed earlier to show that spontaneous breaking of chiral symmetries and the associated massless Goldstone particles arise naturally within the context of strong-coupling lattice gauge theory. Our calculations show the importance of preserving continuous chiral symmetry when transcribing the QCD of massless quarks onto the lattice. The meson sector is analyzed for both one and three spatial dimensions and the criteria for recognizing Nambu-Goldstone phenomena are identified. The relation of these results to continuum QCD and to general properties of observed hadrons is also discussed. In particular the picture which emerges from our discussion leads to a natural understanding of $SU(6)_W$ results when three quark flavors are considered.

Submitted to Physical Review D

---

* Work supported by the Department of Energy under contract number DE-AC03-76SF00515.

1. Introduction

Quantum chromodynamics (QCD) is at present the only attractive candidate for a fundamental theory of hadrons: it provides a basis for understanding the approximate scaling behavior observed at short distances, and recent work strongly suggests that it provides a basis for understanding color confinement.[1,2] However, if QCD is to be a completely satisfactory theory of hadrons it must also account for the observed masses and other physical properties of the hadrons; in particular it must explain the remarkable successes of current algebra combined with the PCAC hypothesis.[3] The study of the emergence of PCAC in the framework of QCD is the focus of this paper. Our goal is to demonstrate that the exact chiral symmetry of the theory in the limit of massless quarks is realized in the hidden, or Nambu-Goldstone (N-G) mode.[4] Specifically we will show that dynamically generated Goldstone bosons arise naturally in strong coupling lattice gauge theories when fermions (quarks) are introduced in a way which preserves the continuous chiral symmetry of continuum QCD. The use of non-perturbative methods is essential for the analysis of the chiral properties even in the strong coupling region; our analysis relies upon iterative block spin techniques developed earlier and successfully applied to a number of simpler problems.[5-8]

The relevance of this strong-coupling lattice result to continuum QCD depends on two properties of non-Abelian lattice gauge theories which have been demonstrated by other workers. Firstly, in the weak-coupling limit and for momenta small compared to the cut-off, the lattice theories reproduce continuum perturbation theory. Secondly, recent calculations[2] by Kogut, Pearson, and Shigemitsu, and by Creutz, for the

theory with no fermions strongly suggest that there is no phase transition between weak and strong coupling regions of this theory. The addition of a small number of fermion flavors should not change this property. Hence we argue that if there are Goldstone bosons in the spectrum of the Hamiltonian at strong coupling they should also be present in the weak coupling theory which is commonly envisioned to contain the continuum limit.

We devote Section 2 of this paper to a review of the physics of spontaneous symmetry breaking, discussing first the continuum U(1) Goldstone theory and second the lattice Heisenberg antiferromagnet. We introduce our calculational technique for detecting spontaneous symmetry breakdown in the context of the latter simple theory, and compare it with a straightforward application of the blocking techniques that we have used previously.

In Section 3 we introduce the lattice QCD Hamiltonian and discuss the strong coupling limit $g^2 >> 1$. We argue that the physics relevant to the dynamical generation of Goldstone bosons is generic to a larger class of theories and subsequently limit our discussion to the case of an Abelian theory. For the sake of simplicity we further restrict our detailed analysis in 3+1 dimensions to the case of a single flavor of fermion. We present our calculations which show that this theory's chiral symmetry is realized in Nambu-Goldstone fashion.[9] These calculations are performed first in the nearest-neighbor approximation to the fermionic gradient operator on the lattice, which has a greater symmetry and hence greater degeneracy in its spectrum. We discuss the way in which longer-range terms in our chirally invariant definition of the gradient lift these degeneracies in the 1+1 dimensional case,

and then present results which confirm the expected generalization for 3+1 dimensions.

In Section 4 we discuss the problem of dynamical mass generation for non-Goldstone particles. We find in our calculation that there are excitations split from the ground state with a gap which is proportional to the inverse lattice spacing. We present a scenario for QCD which suggests that the usual renormalization program would lead to an interpretation of such states as particles of finite mass, such as the vector mesons. We speculate that some interesting properties of hadrons will be natural consequences of this approach, and we discuss the possibility of "seizing"[10] of the U(1) Goldstone bosons in a multiflavor theory.

2. Hidden Symmetries Revisited

In later sections of this paper we will introduce a calculational technique which has proven to be reliable for finding N-G symmetries, if and when they arise. While the method is straightforward, the connection of these ideas to the usual treatments merits discussion.

A. What is a Hidden Symmetry?

The symmetries of a quantum Hamiltonian can be realized in the physics of the theory in either of two ways. The most common situation (and that which must obtain for a finite number of degrees of freedom) is a Wigner realization -- the space of states factors into irreducible representations of the symmetry group. For a system with an infinite number of degrees of freedom there is a second possibility, known in the literature as spontaneous or dynamical symmetry breaking, where the transformations do not exist as unitary operators on the Hilbert space. If the symmetry group is continuous the spectrum of the theory then

contains massless particles. These features arise as a consequence of Goldstone's theorem[4] in a system where a local field acquires a vacuum expectation value which breaks the symmetry. [The existence of a conserved current associated with the symmetry is also a necessary condition of the theorem.] The massless particles are called Goldstone bosons in this event.

This however is not the whole story, for it is possible that this physics (which we call the N-G realization) will appear in a theory through mechanisms other than Goldstone's theorem. Indeed, in one spatial dimension Coleman's theorem[11] tells us that a vacuum expectation value which violates a continuous symmetry can never occur. We will exploit a more general structure to relate the existence of massless particles to conserved local currents.

To explain this way of looking at N-G symmetries we will begin by reviewing some aspects of the physics of such symmetries in the context first of the U(1) Goldstone model and then of the Heisenberg antiferromagnet. Much of this formalism is well known.[12,13] We present it here to stress certain aspects related to the approach to the infinite volume limit, since the lattice techniques used in the analysis of QCD in Section 3 build up to that limit in a stepwise fashion starting from subsystems of finite volume.

B. The U(1) Goldstone Model

This prototypical model is a theory of one complex scalar field. Its Hamiltonian in d spatial dimensions is given by

$$H = \int d^d x \;\; \pi^+\pi + \nabla\phi^+\nabla\phi + V(\phi^+\phi)$$
$$V(z) = \lambda\left(z - \frac{f}{2}\right)^2 \qquad (2.1)$$

Treating H classically, the static field configuration of lowest energy is

$$\phi(\vec{x}) = \frac{1}{\sqrt{2}} f e^{i\theta} \tag{2.2}$$

with θ an arbitrary space-independent constant.

A quantum perturbation theory is formulated by allowing field fluctuations about (2.2) -- i.e., we define

$$\phi(\vec{x}) = \frac{1}{\sqrt{2}} \left(\rho(\vec{x}) + i\chi(\vec{x}) + f e^{i\theta} \right) \tag{2.3}$$

with the vacuum expectation value of $\phi(\vec{x})$ given by

$$\langle \theta | \phi(\vec{x}) | \theta \rangle = \frac{1}{\sqrt{2}} f e^{i\theta} \tag{2.4}$$

where $f \neq 0$ for $d > 1$ dimension. In the infinite volume limit we know that θ parametrizes an infinite set of equivalent, orthogonal, degenerate vacua. The generator of the U(1) group of (phase) transformations under which the Hamiltonian (2.1) is invariant is

$$\begin{aligned} Q &= i\int d^d x \left(\phi(\vec{x})\pi(\vec{x}) - \phi^+(\vec{x})\pi^+(\vec{x}) \right) \\ U(\alpha) &= e^{i\alpha Q} \end{aligned} \tag{2.5}$$

This identifies a conserved current

$$J^\mu(\vec{x}) = i\left(\phi(\vec{x})\partial^\mu\phi^+(\vec{x}) - \phi^+(\vec{x})\partial^\mu\phi(\vec{x}) \right) \tag{2.6}$$

which creates massless χ particles from the $\theta = 0$ vacuum:

$$\langle \chi(\vec{q}); \theta = 0 \mid J^\mu(\vec{x}) \mid \theta = 0 \rangle = \frac{iq^\mu}{\sqrt{2}} f e^{-i\vec{q}\cdot\vec{x}} \tag{2.7}$$

with $q^2 = m_\chi^2 = 0$ by current conservation.

Things are different for finite volume, however. In this case we know that the eigenstates of H must also be eigenstates of the total charge Q. The $|\theta\rangle$ vacua in the infinite volume limit are superpositions of the eigenstates of different Q

$$|\theta\rangle = \frac{1}{\sqrt{2\pi}} \sum_{Q} e^{-i\theta Q}|Q\rangle \tag{2.8}$$

These states have the property

$$U(\alpha)|\theta\rangle = |\theta - \alpha\rangle \tag{2.9}$$

From (2.8) it is evident that the orthogonality and degeneracy of the θ-vacua imply that the energy of the lowest eigenstate of each Q, $\langle Q|H|Q\rangle$, is independent of Q in the infinite volume limit. Hence if we solve for the ground state energy of (2.1) in individual Q sectors we must find that the energies are equal up to terms that vanish as $V \to \infty$.

This point of view also applies in $d = 1$ dimension where Coleman's theorem[11] requires $\langle\phi\rangle = 0$ in (2.4). In this case if we make the dynamical assumption that the lowest states in sectors of definite Q become degenerate in the limit $V \to \infty$, we may form the $|\theta\rangle$ vacua via (2.8).

Since

$$Q|\theta\rangle \equiv \int dx\, J^0(x)|\theta\rangle \neq 0$$

we conclude that $J^0(x)|\theta\rangle \neq 0$ by translation invariance. Then we may define (unnormalized) states with momentum q

$$|q,\theta\rangle = \int dx\, e^{iqx}\, J^0(x)|\theta\rangle \tag{2.10}$$

As $q \to 0$ this becomes $Q|\theta\rangle$ which is orthogonal to $|\theta\rangle$. Defining

$$E(q) = \frac{\langle q,\theta \mid H \mid q,\theta\rangle}{\langle q,\theta \mid q,\theta\rangle} \tag{2.11}$$

we evaluate

$$\lim_{q\to 0} E(q) = \frac{\langle\theta \mid QHQ \mid \theta\rangle}{\langle\theta \mid QQ \mid \theta\rangle} = \frac{\langle\theta \mid QQH \mid \theta\rangle}{\langle\theta \mid QQ \mid \theta\rangle} = E_o \tag{2.12}$$

which is the vacuum energy. Hence there is a sequence of states orthogonal to $|\theta\rangle$ with vanishing energy gap.

We have arrived at the existence of massless states by the back door, via an assumption of degenerate $|Q\rangle$ vacua. Obviously this procedure applies in any number of dimensions; it describes a N-G structure for a continuous symmetry irrespective of the existence of a symmetry-breaking vacuum expectation value for a local field.

C. The Heisenberg Antiferromagnet

We now turn to a discussion of this same physics in the context of a lattice model which has no explicit scalar boson, i.e., the Heisenberg antiferromagnet.[13] We will first discuss the physics as it is known from an exact solution via the Bethe ansatz,[14] and then describe an extension of the block-spin truncation techniques which allows us to recognize this physics correctly. From a computational point of view this extension of the block-spin technique is the important new content of this paper.

The one-dimensional nearest-neighbor Heisenberg antiferromagnet is specified by the Hamiltonian

$$H = J\sum_i \vec{S}_i \cdot \vec{S}_{i+1} \tag{2.13}$$

where $J > 0$, the commutation relations

$$\left[S_i^a, S_j^b\right] = i\,\delta_{ij}\,\epsilon^{abc}\,S_i^c \tag{2.14}$$

and the restriction $\vec{S}_i^2 = 3/4$ for all $\underline{i}$. This restriction to spin-1/2 on each site makes the model inherently quantum, so no classical action or conserved current can be defined; Goldstone's theorem is not applicable. There is however a set of charges which generate rotations of $\vec{S}_i$ under which H is invariant:

$$\begin{aligned} Q^a &= \sum_i S_i^a \\ e^{i\theta^a Q^a}\, S_i^b\, e^{-i\theta^a Q^a} &= R(\vec{\theta})_{bc}\, S_i^c \end{aligned} \tag{2.15}$$

where $R(\theta)$ is a 3×3 rotation matrix. Since

$$\left[Q^a, Q^b\right] = i\,\epsilon_{abc}\,Q^c \tag{2.16}$$

and

$$\left[Q^a, H\right] = 0 \tag{2.17}$$

we may simultaneously diagonalize H, $\vec{Q}^2$, and Q^z.

In the exact solution,[14] it turns out that the lowest states in the various $(\vec{Q}^2, Q^z)$ sectors are all degenerate. Denoting these states by $|\ell,m\rangle$, we may take linear combinations using the spherical harmonics $Y_{\ell m}$

$$|\theta,\phi\rangle = \sum_{\ell,m} Y^*_{\ell m}(\theta,\phi)\,|\,\ell,m\rangle \tag{2.18}$$

in analogy with (2.8). These are the "θ-vacua."

The state $|\theta,\phi\rangle$ is invariant under rotations in the U(1) "little group" of the direction vector with polar angles (θ,ϕ); thus it is annihilated by a certain linear combination $Q_{\theta\phi} = \sum_a \alpha_a(\theta,\phi)Q^a$. The

two orthogonal linear combinations of Q's generate rotations such that

$$e^{i\eta^a Q^a}|\theta,\phi\rangle = |R_\eta(\theta,\phi)\rangle \tag{2.19}$$

analogously to (2.9); the Fourier components of their densities create two Goldstone bosons via (2.10).

To be more concrete, say we choose to build our theory on the $|\theta = 0,\phi = 0\rangle$ vacuum. Then $Y_{\ell m}(0,0) = \sqrt{(2\ell+1)/4\pi}\,\delta_{m,o}$ so $Q^z|0,0\rangle = 0$ as promised. Further, Q^x and Q^y change m, so they do not annihilate the vacuum. Thus a U(1) subgroup of SU(2) is realized in the Wigner mode, and the massless excitations generated by $\sum_n e^{iqn}\left(S^x_n \pm iS^y_n\right)$ have the $Q^z = \pm 1$ quantum numbers of $Q^x \pm iQ^y$. Hence the 1 + 1 dimensional Heisenberg antiferromagnet exhibits a degeneracy structure like that of the 1 + 1 dimensional U(1) Goldstone model.

In the standard lattice truncation procedure[6] we would construct a trial wave function by diagonalizing that part of the Hamiltonian which refers only to a block of n sites and writing block-to-block recoupling terms as operators among a restricted set of states -- the lowest few -- on the n site blocks. This method automatically constructs states which respect the symmetries of the Hamiltonian,[15] namely in this case states of definite $|\ell,m\rangle$. Keeping only a few such states makes it difficult to recognize a spontaneously broken symmetry since as we have shown this is signalled by an infinite set of degenerate $|\ell,m\rangle$ eigenstates in infinite volume. We describe here a variant of the procedure which constructs the variational wave function by diagonalizing on n sites not the symmetric Hamiltonian (2.15), but a Hamiltonian to which a symmetry-breaking perturbation has been added

$$H(\varepsilon) = J \sum_i \vec{S}_i \cdot \vec{S}_{i+1} + \varepsilon \sum_i S_i^z S_{i+1}^z \qquad (2.20)$$

and again keeping a restricted set of states on each block. If spontaneous symmetry breaking occurs then we would expect that the ground state expectation value of the symmetric Hamiltonian would minimize for distorted states constructed from $H(\varepsilon)$ with $\varepsilon \neq 0$, and indeed this is exactly what happens.[16] The states constructed by this method are not $|\ell,m\rangle$ eigenstates: rather, the algorithm constructs directly a state of the $|\theta,\phi\rangle$ type. To see that there is an infinite number of degenerate states of this type we need only remark that the charges Q_x and Q_y, which commute with (2.13), generate rotations which change the direction of the perturbation in (2.20). For any such rotated perturbation the truncation method constructs a trial state degenerate with the one constructed from (2.20), since the Hamiltonian (2.13) is symmetric. That the states constructed for different (θ,ϕ), that is, for different directions selected by the perturbing term in (2.22), are orthogonal will be shown in detail for the QCD case in Section 3.[17]

3. Goldstone Bosons in the Lattice Gauge Theory

In this section we will present a discussion of our calculations for QCD. We begin with a chirally invariant Hamiltonian for a multi-flavored non-Abelian lattice gauge theory. In studying the strong coupling limit of this Hamiltonian we simplify to a single flavor, and employ the iterative lattice truncation procedure. We examine first the $1+1$ dimensional case and then generalize our results to higher dimensions.

A. Formalism

In the Hamiltonian approach it is convenient to work in the gauge $A_0 = 0$. As with Gauss' law in QED, the non-Abelian generalization of Gauss' law is not an equation of motion in this gauge. We impose it as a condition on the states -- namely that they transform as singlets under all local gauge transformations. We follow the Wilson-Kogut-Susskind formulation[1] of a lattice gauge theory.[18] As has been discussed at length elsewhere, we introduce fermions in a way which explicitly maintains continuous chiral symmetry and gives the correct spectrum for a free Dirac particle in the zero coupling limit.[5] This is achieved by using a long-range form for the derivative

$$\partial_\mu \psi_{\vec{j}} = \frac{1}{a} \sum_n \delta'(n)\, \psi_{\vec{j}+n\hat{\mu}} \tag{3.1}$$

where

$$\delta'(n) = \frac{1}{2N+1} \sum_{m=-N}^{N} ik(m)\, e^{ik(m)\cdot n} \underset{N\to\infty}{\to} \frac{(-1)^{n+1}}{|n|}$$
$$k(m) = \frac{2\pi m}{2N+1} \tag{3.2}$$

The Hamiltonian for coupling strength g and lattice spacing a is then

$$H(g,a) = \frac{1}{a}\left\{ \sum_{\text{links}} \frac{1}{2} g^2 E^{\alpha 2}_{\vec{j},\hat{\mu}} - \sum_{\text{loops}} \frac{1}{g^2} \mathrm{Tr}\left[\prod_{\substack{\text{around}\\ \text{loop}}} U_{\vec{j},\hat{\mu}} \right] \right.$$
$$\left. - \left[i \sum_{\substack{\vec{j},\hat{\mu}\\ n>0}} \delta'(n)\, \psi^{+\alpha f}_{\vec{j}}\, \alpha_\mu\, \psi^{\beta f}_{\vec{j}+n\hat{\mu}} \left[\prod_{m=0}^{n-1} U_{\vec{j}+m\hat{\mu},\hat{\mu}} \right]^{\alpha\beta} + \text{h.c.} \right] \right\} \tag{3.3}$$

We have introduced here a four component fermion field $\psi^{\alpha f}_{\vec{j}}$ for each color, α, and flavor, f, at each site $\vec{j}$. The α_μ are the usual Dirac matrices. The operators $U_{\vec{j},\hat{\mu}}$ create unit color flux on the link joining the site $\vec{j}$ to the site $\vec{j}+\hat{\mu}$. The operators $E_{\vec{j},\hat{\mu}}$ measure this flux excitation. In our notation the only dimensionful quantity is the lattice spacing a, which thus appears only as an overall scale factor for the Hamiltonian. The Hamiltonian (3.3) in the limit $g \to 0$ reduces to a massless, chirally invariant, free Dirac theory which has a spectrum $E_{\vec{k}} = |\vec{k}|$. The Hamiltonian commutes with the chiral charges

$$Q_5^\eta = \sum_{\vec{j}} \psi^{+\alpha f}_{\vec{j}} (\lambda^\eta)^{ff'} \gamma_5 \psi^{\alpha f'}_{\vec{j}} \tag{3.4}$$

where the λ^η are the generator matrices of the flavor group.

At strong coupling the gauge invariant states of the system described by H fall into two classes: those containing flux excitations, which all have energy proportional to g^2, and those involving no flux excitations, which, by Gauss' law, may contain only color-singlet fermionic configurations at any individual site. There is a huge degenerate set of such states having zero energy (to zeroth order in $1/g^2$). Acting on any such state the fermionic term in (3.3) creates at least one excited flux link; however, allowing the fermionic term in H to act twice, we can mix states within the zero flux sector and split the degeneracy by creating and subsequently annihilating flux links, as shown in the examples of Fig. 1. The zeroth-order color-singlet excitations thus move through space or exchange flavor by passing through intermediate states in the highly excited sector containing flux.

In order to construct trial wave functions for the low lying eigenstates of H we restrict our attention to the fluxless states. The above remarks make it clear that degenerate perturbation theory leads us to diagonalize an effective second order Hamiltonian. This will give the leading term of a $1/g^2$ expansion which has the form

$$H^{(2)}_{eff} = \frac{\Lambda^2}{N_c} \sum_{\vec{j},n,\mu} \frac{\delta'(n)\delta'(-n)}{\frac{1}{2}g^2 \Lambda|n| C_F} \psi^{+\alpha f}_{\vec{j}} \alpha_\mu \psi^{\beta f}_{\vec{j}+n\hat{\mu}} \psi^{+\beta f'}_{\vec{j}+n\hat{\mu}} \alpha_\mu \psi^{\alpha f'}_{\vec{j}} \qquad (3.5)$$

where N_c = number of colors; C_F is the value of the quadratic Casimir operator of $SU(N_c)$ in the fundamental representation, and $\Lambda = 1/a$.

The denominator $\frac{1}{2}g^2 \Lambda|n|C_F$ is the energy of an intermediate state containing $\underline{n}$ excited flux links. Were we to discuss the baryon spectrum in color SU(3) we would need to keep terms at least up to order $1/g^4$ in order to have terms in H_{eff} which could move a qqq excitation. Baryon-meson interchange interactions also enter at order $1/g^4$. However, we can consistently treat the meson sector of the theory on the basis of $H^{(2)}_{eff}$ and hence in the remainder of this paper we discuss a lattice truncation calculation of its spectrum.

It is convenient to rewrite (3.5) by performing a Fierz transformation which groups together the operators corresponding to a single site. This gives

$$H^{(2)}_{eff} = -\frac{\Lambda}{2g^2 C_F} \sum_{\vec{j},n,\hat{\mu}} \frac{\delta'(n)\delta'(-n)}{|n|} \left[\sum_{\eta=1}^{16} \left(\frac{1}{\sqrt{N_c}} \psi^{\alpha f}_{\vec{j}} M^\eta \psi^{\alpha f'}_{\vec{j}} \right) \right.$$

$$\left. \times \left(\frac{1}{\sqrt{N_c}} \psi^{\beta f'}_{\vec{j}+n\hat{\mu}} \alpha_\mu M^\eta \alpha_\mu \psi^{\beta f}_{\vec{j}+n\hat{\mu}} \right) + \frac{1}{N_c} \psi^{+\alpha f}_{\vec{j}} \psi^{\alpha f}_{\vec{j}} \right] \qquad (3.6)$$

where the M^η are the 16 Hermitian 4×4 matrices listed in Table I.

Because of our restriction to purely mesonic configurations the last term in (3.6) is a trivial constant, and hence can be dropped. It is also clear at this point that color enters (3.6) in a totally trivial fashion. We may consequently suppress the color indices. The resulting Hamiltonian can be viewed as the strong coupling limit of a compact lattice formulation of an Abelian gauge theory, the restriction to color singlet excitations at each site replaced by a restriction to states with fermion number everywhere zero. As a simplification we will discuss the case of a single flavor. Then the term involving $M^{16} = \mathbf{I}$ in (3.6) is also a constant which can be ignored. After detailed discussion of this problem we will make some comments on theories with multiple flavors and colors (see Section 4).

Our discussion will be given in two stages. First, we consider a nearest-neighbor theory obtained by dropping all terms $n > 1$ in (3.6). This fictitious theory has an SU(4) symmetry: not only the axial charge

$$Q_5 = \sum_{\vec{j}} \psi^{+}_{\vec{j}} \gamma_5 \psi_{\vec{j}} \tag{3.7}$$

but the entire set of 15 charges

$$Q^{\eta} = \sum_{\vec{j}=(j_x,j_y,j_z)} \psi^{+}_{\vec{j}} \alpha_x^{j_x} \alpha_y^{j_y} \alpha_z^{j_z} M^{\eta} \alpha_z^{j_z} \alpha_y^{j_y} \alpha_x^{j_x} \psi_{\vec{j}} = \sum_{\vec{j}} Q^{\eta}_{\vec{j}} \tag{3.8}$$

commutes with the Hamiltonian. The six chargeless states which can be formed on a single site (listed in Table II) form an irreducible multiplet of the SU(4) symmetry: we can write the $Q^{\eta}_{\vec{j}}$ in the basis of these sextets. This additional symmetry means additional degeneracy in the spectrum of the nearest neighbor case, since (at least in finite volume) the states must fall into multiplets of the SU(4).

To study the physics of the Nambu-Goldstone mode and also to learn how these extra degeneracies are lifted when long-range terms are restored we have studied in detail the $1+1$ dimensional theory. This theory is a lattice version of the SU(2) Schwinger model,[19] since the degrees of freedom which represent spin in a $3+1$ dimensional theory must be interpreted as an internal (flavor) degree of freedom in the $1+1$ dimensional case. The calculations presented in this section study first this $1+1$ dimensional theory for the nearest-neighbor case. Then longer-range interactions are reintroduced. (In $1+1$ dimensions even the long-range theory has an $SU(2) \times SU(2) \times U(1)$ symmetry, where the U(1) is given by the Q^x formed using $M = \alpha_x$ and the $SU(2) \times SU(2)$ are a V+A and V-A formed from the six Q^η which commute with Q^x. This is just the chiral symmetry of the SU(2) Schwinger model.)

We find that the axial symmetries of the $1+1$ dimensional model are realized in Nambu-Goldstone mode. In itself, of course, this result is nothing new, in view of what is known about the SU(2) Schwinger model. Its importance lies rather in the fact that its extension to $3+1$ dimensions is easily conceived and leads to the conclusion that chiral symmetry in the strong-coupling lattice theory is associated with Goldstone bosons.

Our iterative truncation scheme will be reviewed as we apply it to the nearest-neighbor version of (3.6), from which we will deduce a simple scenario for symmetry realization in the long-range theory. This scenario has been verified explicitly both for the $1+1$ dimensional case and for the $3+1$ dimensional case.

B. Nearest-Neighbor Theory

(i) Block-spin transformation, 1+1 dimensions

Keeping only nearest-neighbor terms in (3.6) we get

$$H_{nn}^{(2)} = \frac{4}{g^2} \sum_j \vec{Q}_j \cdot \vec{Q}_{j+1} \tag{3.9}$$

The Q_j^α are SU(4) generators in the $\underline{6}$ representation; the Hamiltonian is just that of an SU(4) antiferromagnet.

In order to effect a block-spin transformation, we divide the lattice into blocks of three sites each. (Figure 2; the reason for blocking in threes will soon be apparent.) We then group the terms in the Hamiltonian according to whether they act entirely within blocks or connect adjacent blocks:

$$\begin{aligned} \frac{g^2}{4} H_{nn}^{(2)} &= \sum_p H_p + \sum_p H_{p,p+1} \\ H_p &= \vec{Q}_{p1} \cdot \vec{Q}_{p2} + \vec{Q}_{p2} \cdot \vec{Q}_{p3} \\ H_{p,p+1} &= \vec{Q}_{p3} \cdot \vec{Q}_{p+1,1} \end{aligned} \tag{3.10}$$

Here $\underline{p}$ indexes blocks and $\underline{1}$, $\underline{2}$, $\underline{3}$ index sites within a block.[20] The idea is to diagonalize the H_p's, which commute with one another, and to truncate the Hilbert space basis to products of the lowest-lying states in the blocks. $\bar{H}_{p,p+1}$ is then rewritten in the truncated basis, yielding an effective Hamiltonian operating on the low-lying block states.

To accomplish this we rewrite

$$H_p = \frac{1}{2}\left(\vec{Q}_p^T\right)^2 - \frac{1}{2}\left(\vec{Q}_p^+\right)^2 - \frac{1}{2}\left(\vec{Q}_{p2}\right)^2 \tag{3.11}$$

where

$$\vec{Q}_p^{+} = \vec{Q}_{p1} + \vec{Q}_{p3}$$
$$\vec{Q}_p^{T} = \vec{Q}_p^{+} + \vec{Q}_{p2} \qquad (3.12)$$

Diagonalization of H_p proceeds in a way reminiscent of $\vec{L}\cdot\vec{S}$ coupling in atomic physics. To wit, we note that the operators $(\vec{Q}^T)^2$ and $(\vec{Q}^+)^2$ may be diagonalized simultaneously, along with the three SU(4) "magnetic" quantum numbers of $\vec{Q}^T$. $\left[(\vec{Q}_2)^2\right.$ is already a c-number, the Casimir operator in the sextet.$\left.\right]$ We first couple $\vec{Q}_1$ and $\vec{Q}_3$ to states of definite $(\vec{Q}^+)^2$, and then we couple $\vec{Q}^+$ and $\vec{Q}_2$ to definite $(\vec{Q}^T)^2$. The combination of representations is depicted in Fig. 3. Now we note that (3.11) demands that we maximize $(\vec{Q}^+)^2$ and minimize $(\vec{Q}^T)^2$ -- just the behavior one would expect in an antiferromagnet. The coupling scheme for the low-lying states is then

$$\vec{Q}_1 + \vec{Q}_3 = \vec{Q}^+ \; : \; \underline{6} \times \underline{6} \rightarrow \underline{20}$$
$$\vec{Q}^+ + \vec{Q}_2 = \vec{Q}^T \; : \; \underline{20} \times \underline{6} \rightarrow \underline{6} \qquad (3.13)$$

The block states of lowest energy form a sextet, just like the states on each site; this is the reason we blocked together three sites.

The energy per block in the configuration (3.13) is computed from (3.12) using the values listed in Fig. 3 for the Casimir operator. We get an energy density (per block)

$$E_o = -\frac{4}{g^2} \cdot 6 \qquad (3.14)$$

Taking only the lowest sextet in each block to form our truncated basis, we evaluate matrix elements of $\vec{Q}_{pi}$ with the Wigner-Eckart theorem:

$$\langle \underline{6m} \mid \vec{Q}_{pi} \mid \underline{6m'} \rangle = \gamma_i \langle \underline{6m} \mid \vec{Q}_p^T \mid \underline{6m'} \rangle \tag{3.15}$$

with $\gamma_1 = \gamma_3 = 3/5$, $\gamma_2 = -1/5$. Thus in the truncated Hilbert space each H_p is replaced by E_o and

$$H_{p,p+1} = \vec{Q}_{p3} \cdot \vec{Q}_{p+1,1} \rightarrow \frac{9}{25} \vec{Q}_p^T \cdot \vec{Q}_{p+1}^T \tag{3.16}$$

Dropping T superscripts, the truncated Hamiltonian is then

$$H_1^{Tr} = \frac{N}{3} E_o + \frac{4}{g^2} \cdot \frac{9}{25} \sum_{\vec{p}} \vec{Q}_p \cdot \vec{Q}_{p+1} \tag{3.17}$$

and the transformation is complete and ready to be iterated. Writing the effective Hamiltonian after $\underline{n}$ iterations as

$$H_n^{Tr} = \frac{4}{g^2} \left(N\alpha_n + \beta_n \sum_p \vec{Q}_p \cdot \vec{Q}_{p+1} \right) \tag{3.18}$$

we deduce the recursion relations

$$\begin{aligned} \alpha_n &= \alpha_{n-1} - \frac{6}{3^n} \beta_{n-1} \\ \beta_n &= \frac{9}{25} \beta_{n-1} \end{aligned} \tag{3.19}$$

where $\alpha_0 = 0$ and $\beta_0 = 1$.

It is now trivial to demonstrate that to the accuracy of this calculation the nearest-neighbor theory has no mass gap. Suppose that the gap to the first excited state of (3.9) is Δ. Then the equivalent gap for (3.17) is $(9/25)\Delta$ since the two Hamiltonians differ solely in scale. Because we expect (3.17) to describe the low-energy physics of the theory fairly well, we equate $\Delta = (9/25)\Delta$ to get $\Delta = 0$. Possible <u>massive</u> excited states are probably lost together with high-momentum modes in the truncation.

To show that the vanishing mass gap is associated with N-G phenomena, we consider doing some large number of iterations in the manner described. Our effective Hamiltonian is (3.18), with β_n exceedingly small. Now we dissect the lattice into blocks of two sites each and decompose H_n^{Tr} in a fashion analogous to (3.10). Then

$$H_p = \vec{Q}_{p1} \cdot \vec{Q}_{p2} = \frac{1}{2}\left(\vec{Q}_p^T\right)^2 - \frac{1}{2}\left(\vec{Q}_{p1}\right)^2 - \frac{1}{2}\left(\vec{Q}_{p2}\right)^2 \qquad (3.20)$$

with

$$\vec{Q}_p^T = \vec{Q}_{p1} + \vec{Q}_{p2} \qquad (3.21)$$

We are called upon to minimize the value of $(\vec{Q}^T)^2$, and a glance at Fig. 3(a) shows that the ground state of H_p is the SU(4) singlet. It is reasonable to attempt to construct a unique vacuum by taking a state where each block is in this singlet state. Of course $H_{p,p+1}$ has no matrix element within this ground state, but if we create an excited state by putting one block into a member of the 15 then $H_{p,p+1}$ moves it around to form a momentum band (and creates more complicated states). It seems, then, that the ground state of (3.18) is SU(4)-invariant while low-lying excited states transform as a 15 and have mass of the order of β_n.

However, if we picture progressively deferring the change-over from three-site to two-site blocking, β_n may be made arbitrarily small. Taking it indeed to be zero, we find an infinite set of ground states consisting of a singlet, a 15, the representations contained in $15 \times 15 \supset 20 + 45 + 45 + \ldots$ and so forth. By combining enough of these representations along the lines of (2.18) the "θ-vacua" may be constructed,

which will realize some or all of the symmetry generators in N-G mode.

Some further insight into the nature of the spectrum of this theory can be gained by considering the effect of adding a small fermion mass to (3.3). This yields in perturbation theory (assuming $m << 1/g^2$)

$$H_m = \frac{4}{g^2} \sum_j \vec{Q}_j \cdot \vec{Q}_{j+1} + 2m \sum_j (-1)^j Q_j^M \qquad (3.22)$$

where Q_j^M is the charge associated with the $M^\eta = \beta = \gamma_o$ generator. The addition of this term breaks the SU(4) symmetry down to $SU(2) \times SU(2) \times U(1)$ as shown in Table III; the set of 6 single-site states consists of a $(\frac{1}{2}, \frac{1}{2})^0$, a $(0,0)^{+1}$, and a $(0,0)^{-1}$ under this symmetry. A truncation calculation for this Hamiltonian -- keeping one $(\frac{1}{2}, \frac{1}{2})$ multiplet and two (0,0) multiplets at each step -- has been carried out. As in the symmetric case the site-to-site coupling term is reduced in strength at each iteration so that eventually the mass term dominates, even for very small $\underline{m}$. The theory has a unique ground state of the (0,0) type; the lowest excited state is of the $(\frac{1}{2}, \frac{1}{2})$ type and is split from the ground state. The charges Q^η which do not commute with Q^M (those listed below the line in Table III) transform as a $(\frac{1}{2}, \frac{1}{2})$ multiplet, and we can write in analogy to (2.7)

$$\langle \tfrac{1}{2}, \tfrac{1}{2}; q \mid Q_j^\eta \mid 0,0 \rangle = \frac{i}{\sqrt{2}} f(q) \, e^{-iqj} \qquad (3.23)$$

where $\underline{q}$ is the momentum of the $(\frac{1}{2}, \frac{1}{2})$ state. As we take $\underline{m}$ to zero (and these charges become conserved) the $(\frac{1}{2}, \frac{1}{2})$ particles become massless[21] -- the symmetry is realized in the Nambu-Goldstone fashion. If the symmetry were Wigner-realized then in this limit the splitting would remain finite and $\underline{f}$ would go to zero. The results of our calculation

indicate that this is not the case. We note however that the $SU(2) \times SU(2) \times U(1)$ algebra of conserved charges which commute with Q^M is Wigner-realized.

(ii) Higher dimensions

The extension of the nearest-neighbor analysis to two and three dimensions is straightforward. A simple SU(4)-symmetric block-spin transformation on 3^d sites may be constructed by working one dimension at a time (see Fig. 4). It is readily demonstrated that the Hamiltonian (3.9) still scales, with a factor of $9 \cdot 19/25 \cdot 25$ in two dimensions and $9 \cdot 19 \cdot 19/25 \cdot 25 \cdot 25$ in three dimensions. Hence the 3+1 dimensional theory is massless and θ-vacua may be constructed as before, either by blocking 2^3 sites or by perturbing with a mass term.

While it happens that no x-y-z asymmetry is introduced in the effective Hamiltonian by this blocking scheme, for the non-nearest-neighbor case this will not be so. We have confirmed the result obtained here by an alternate procedure which manifestly respects x-y-z symmetry. We will describe this method in some detail for two spatial dimensions and then outline the obvious generalization to three spatial dimensions.

On the block of nine sites in two spatial dimensions we consider first the nearest-neighbor Hamiltonian for the five sites enclosed by the dotted line in Fig. 5. It is

$$H_{5\text{-site}} = \frac{1}{2} \sum_{n=1}^{15} \left(Q^n_{00} + Q^n_{01} + Q^n_{0-1} + Q^n_{-10} + Q^n_{10} \right)^2 - Q^{n2}_{00} - \left(Q^n_{01} + Q^n_{0-1} + Q^n_{10} + Q^n_{-10} \right)^2 \tag{3.24}$$

As was the case for the three-site Hamiltonian, one can readily read off

from this expression the desired representation content for the lowest-lying states on the five sites: it would be a maximal representation, namely the totally symmetric 105-dimensional representation, for the four outside sites, contracted with the sextet on the center site in such a way as to reduce the dimension as much as possible, namely to a $\underline{50}$. The relevant Young tableaux are shown in Fig. 6(a). Let us denote these states ψ_i^{50} where $\underline{i}$ indexes the 50 states.

We truncate to this multiplet and reintroduce the couplings to the four corner sites of the nine-site square. We define

$$\hat{Q}^\eta = \left(Q^\eta_{01} + Q^\eta_{10} + Q^\eta_{0-1} + Q^\eta_{-10} \right) \tag{3.25}$$

and remark that the symmetry of the $\underline{105}$ in ψ^{50} gives

$$\langle \psi_i^{50} \mid Q^\eta_{01} \mid \psi_j^{50} \rangle = \langle \psi_i^{50} \mid Q^\eta_{10} \mid \psi_j^{50} \rangle = \ldots = \frac{1}{4} \langle \psi_i^{50} \mid \hat{Q}^\eta \mid \psi_j^{50} \rangle \tag{3.26}$$

Furthermore we can use the Wigner-Eckart theorem to show that

$$\langle \psi_i^{50} \mid \hat{Q}^\eta \mid \psi_j^{50} \rangle = \frac{8}{7} \langle \psi_i^{50} \mid \hat{Q}^\eta + Q^\eta_{00} \mid \psi_j^{50} \rangle \equiv \frac{8}{7} \langle \psi_i^{50} \mid Q^\eta_{50} \mid \psi_j^{50} \rangle \tag{3.27}$$

The coefficient 8/7 is simply a ratio of Clebsch-Gordan coefficients. The couplings of the corner sites to the $\underline{50}$ can then be written as

$$\begin{aligned} \Delta H &= -\frac{1}{2} \cdot \frac{8}{7} \sum_\eta Q^\eta_{50} \left(Q^\eta_{11} + Q^\eta_{1-1} + Q^\eta_{-11} + Q^\eta_{-1-1} \right) \\ &= \frac{2}{7} \sum_\eta \left\{ \left(Q^\eta_{50} + Q^\eta_{\text{corner}} \right)^2 - Q^{\eta 2}_{50} - Q^{\eta 2}_{\text{corner}} \right\} \end{aligned} \tag{3.28}$$

where

$$Q^\eta_{\text{corner}} = Q^\eta_{11} + Q^\eta_{1-1} + Q^\eta_{-11} + Q^\eta_{-1-1}$$

The lowest lying eigenstates of (3.28) are again obvious -- we must form a symmetric 105 from the four corner sites and combine it with the 50 to form the smallest possible overall representation which is a sextet. Figure 6(b) shows the relevant Young tableaux. We have thus a two-step algorithm which produces trial states on nine-site block which have the same group structure as the states on a single site and which furthermore are obviously invariant under 90^{o} rotations.

The generalization of this procedure to three dimensions is quite obvious and works in a similar fashion. We begin by constructing the multiplet on the seven sites (000), (001), (00-1), (010), (0-10), (100), and (-100) which is represented by the Young tableau in Fig. 7(a). Next we truncate to this multiplet and reintroduce the couplings to the 12 sites which are at the centers of the edges of the cube. We find that the lowest states for this system comprise a completely symmetric multiplet on the 12 edge centers coupled as shown in Fig. 7(b) to the states described in Fig. 7(a). Finally we take these states and reintroduce the couplings to the eight corners of the cube. Again we find the lowest multiplet to be a completely symmetric representation on these eight sites combined with the state of Fig. 7(b) to give a sextet. Clearly this procedure can then be repeated since we have now arrived at an effective block Hamiltonian of the same form as the Hamiltonian with which we started which acted on the site sextets, namely $\beta \sum Q^{\eta}(\vec{p})Q^{\eta}(\vec{p}+\hat{\mu})$. To complete the SU(4) calculation we have only to calculate the coefficient in front of this new Hamiltonian. It is clearly a number less than one, which is sufficient information to verify that the nearest-neighbor theory has a massless excitation spectrum.

C. Long-Range Interactions

At attractive picture of symmetry realization in the non-nearest-neighbor theory follows from consideration of Table III. We have argued that in the θ vacuum selected by the mass term the nearest-neighbor theory (in any number of dimensions) exhibits a symmetry pattern wherein the SU(4) charges which commute with Q^M (those above the line) are in Wigner mode whereas those which do not (below the line) are in N-G mode. Putting in the long-range gradient for $d = 1$ breaks eight of the SU(4) generators (see Table IV); of the surviving seven, some lie above the line in Table III and some below. It is tempting to conclude that those above are still Wigner-realized (these are the "V" generators of Table IV) and those below still N-G. Similarly, for $d = 3$, where Q_5 is the only surviving symmetry generator, the fact that it lies below the line in Table III suggests that chiral symmetry in three dimensions is found in an N-G realization.

Alternatively, it is quite possible that inclusion of the symmetry-breaking long-range terms changes drastically the nature of the vacuum and the realization of symmetries in the Fock space. We will check explicitly that this does not happen.

Our long-range Hamiltonian (3.6) in one dimension is

$$H_{eff}^{(2)} = \frac{4}{g^2} \sum_{\substack{j,\eta \\ n>0}} \frac{1}{n^3} (s_\eta)^{n+1} Q_j^\eta Q_{j+n}^\eta \tag{3.29}$$

where $s_\eta = +1$ for those charges above the line in Table IV and $s_\eta = -1$ for those below. Since it is unlikely that distant interactions weighted with $1/n^3$ can affect the physics once we have enough terms to break SU(4), a simplification suggests itself: we will retain interactions

only as far as n = 2, approximating $H_{eff}^{(2)}$ with[22]

$$H = \frac{4}{g^2}\left\{\sum_{j_1} \vec{Q}_j \cdot \vec{Q}_{j+1} + \frac{1}{8}\sum_{j,\eta} s_\eta \, Q_j^\eta \; Q_{j+2}^\eta\right\} \tag{3.30}$$

The Hamiltonians (3.29)-(3.30) are symmetric under the SU(2) × SU(2) × U(1) displayed in Table IV, which is distinct from the SU(2) × SU(2) × U(1) left by the mass perturbation of the previous section. However the same decomposition applies for the elementary sextet of states on each site.

A simple blocking scheme would proceed as in the nearest-neighbor theory. Grouping three sites together according to

$$H_p = \vec{Q}_{p1} \cdot \vec{Q}_{p2} + \vec{Q}_{p2} \cdot \vec{Q}_{p3} + \frac{1}{8}\sum_\eta s_\eta \, Q_{p1}^\eta \; Q_{p3}^\eta \tag{3.31}$$

$$H_{p,p+1} = \vec{Q}_{p3} \cdot \vec{Q}_{p+1,1} + \frac{1}{8}\sum_\eta s_\eta\left(Q_{p2}^\eta Q_{p+1,1}^\eta + Q_{p3}^\eta Q_{p+1,2}^\eta\right) \tag{3.32}$$

we would diagonalize the block Hamiltonian H_p and select the lowest eigenstates in each of the SU(2) × SU(2) × U(1) sectors of a single site SU(4) sextet. Truncation of the operators in the block-block coupling term $H_{p,p+1}$ to these states would yield a new effective Hamiltonian.

It is our expectation that at least some of the symmetries of (3.30) will be realized in N-G mode; in particular, we foresee that the θ vacuum which is selected by a mass perturbation will not permit the axial generators (α_x and "A'" in Table IV) to appear in Wigner realization. In this light it makes sense to choose block states which result from distorting the low-lying eigenstates of H_p so as to break these generators, as discussed for the Heisenberg model in Section 2.

To distort the eigenstates of H_p we define a distorted block Hamiltonian

$$H_\varepsilon = H_p + \varepsilon\left(Q^M_{p1}Q^M_{p2} + Q^M_{p2}Q^M_{p3} - \frac{1}{8}\,Q^M_{p1}Q^M_{p3}\right) \tag{3.33}$$

which differs from H_p in that the Q^M term is strengthened; this breaks the axial generators. H_ε is to be used only to define the block states to which we will truncate in the first iteration: the effective Hamiltonian which couples blocks will be derived by taking matrix elements of the original, undeformed block-block Hamiltonian $H_{p,p+1}$ in the truncated basis. ε is a variational parameter.

Thus for our block states we take the six low-lying eigenstates[23] $|i_\varepsilon\rangle$ of H_ε and evaluate the ground-state energy

$$E_o \equiv \langle 0_\varepsilon | H_p | 0_\varepsilon \rangle \tag{3.34}$$

the local splitting term

$$\left(H^L_p\right)_{ij} = \langle i_\varepsilon | H_p | j_\varepsilon \rangle - E_o\,\delta_{ij} \tag{3.35}$$

and matrix elements of the local charges

$$\begin{aligned}
\left(\vec{Q}_L\right)_{ij} &\equiv \langle i_\varepsilon | \vec{Q}_{p1} | j_\varepsilon \rangle && \text{(left)} \\
\left(\vec{Q}_C\right)_{ij} &\equiv \langle i_\varepsilon | \vec{Q}_{p2} | j_\varepsilon \rangle && \text{(center)} \\
\left(\vec{Q}_R\right)_{ij} &\equiv \langle i_\varepsilon | \vec{Q}_{p3} | j_\varepsilon \rangle = \left(\vec{Q}_L\right)_{ij} && \text{(right)}
\end{aligned} \tag{3.36}$$

where the last equality follows from left-right symmetry. Then the truncated Hamiltonian takes the form

$$\begin{aligned}
\frac{g^2}{4} H_1^{Tr} = \frac{N}{3} E_o + \sum_p H^L_p + \sum_p \Big\{ & \vec{Q}_{Rp} \cdot \vec{Q}_{Lp+1} \\
& + \frac{1}{8} \sum_\eta s_\eta \left(Q^\eta_{Cp} Q^\eta_{Lp+1} + Q^\eta_{Rp} Q^\eta_{Cp+1} \right) \Big\}
\end{aligned} \tag{3.37}$$

Each of the new sites (old blocks) has two sets of 15 operators associated with it: $\vec{Q}_C$ and $\vec{Q}_L = \vec{Q}_R$. The next iteration proceeds in a like manner, without making it necessary to introduce yet more operators per site. We note that the distorted H_ε need be used only in the first iteration: the asymmetry in the block states introduces an asymmetry in the $\vec{Q}_L$ and $\vec{Q}_C$ matrices through (3.36) when the truncation is performed, and this propagates the distortion through further iterations.

This calculation has been carried out on a computer. Each iteration has as input data the explicit 6×6 matrices representing $\vec{Q}_L$, $\vec{Q}_C$, and H^L in some basis for the site states; direct products of the basis states on three sites are constructed and the matrix elements of H_p (and of H_ε in the first iteration) are calculated; finally low-lying eigenstates of H_p (or H_ε) are found and matrix elements of $\vec{Q}_L$, $\vec{Q}_C$, and H^L are calculated among them. At the same time the variational ground-state energy density is accumulated. We find that the energy density is minimized for $\varepsilon \neq 0$. This confirms the N-G realization of the axial currents as follows:

We have denoted the block states which emerge from the first iteration as $|i_\varepsilon\rangle$; recall that they are eigenstates of H_ε. Truncating the Hilbert space basis to these states means that the variational ground state which we will eventually construct is some linear combination of products of these block states:

$$|0\rangle = \sum_{\{i_n\}} a_{\{i_n\}} \prod_n |i_\varepsilon\rangle_n \tag{3.38}$$

Here n indexes blocks of the lattice and the a's are coefficients determined in the iterative process. Consider now an SU(4) rotation operator

constructed with one of the axial generators (3.8)

$$U = e^{i\theta Q^{\alpha}} \tag{3.39}$$

If we use

$$H_{\varepsilon}^{\theta} \equiv U H_{\varepsilon} U^{-1} \tag{3.40}$$

to define deformed block states $|i_{\varepsilon}^{\theta}\rangle$ in the first iteration then these states are related to the ones in (3.38) by

$$|i_{\varepsilon}^{\theta}\rangle = U|i_{\varepsilon}\rangle \tag{3.41}$$

Obviously the variational ground state that will be constructed eventually is

$$|0^{\theta}\rangle = \sum_{\{i_n\}} a_{\{i_n\}} \prod_n |i_{\varepsilon}^{\theta}\rangle_n = U|0\rangle \tag{3.42}$$

Since U is unitary, we have

$$\langle i_{\varepsilon} | j_{\varepsilon}^{\theta}\rangle = N_{ij} < 1 \tag{3.43}$$

so that

$$\langle 0 | 0^{\theta}\rangle = \sum_{\{i_n\}} \sum_{\{j_n\}} a^{*}_{\{i_n\}} a_{\{j_n\}} \prod_n N_{i_n j_n} \to 0 \tag{3.44}$$

exponentially in the volume.[24] $SU(2) \times SU(2) \times U(1)$ invariance implies that $|0\rangle$ and $|0^{\theta}\rangle$ have the same energy; thus we have explicitly displayed a variational approximation to the family of θ-vacua of the model. The "V" generators of Table IV commute with the deformation terms in (3.33) and hence with H_{ε} as well as with the real Hamiltonian: they annihilate the variational vacua and are Wigner-realized.

We have performed a similar computer calculation for the three-dimensional non-nearest-neighbor problem by executing 3-site blockings

in the x, y and z directions, successively. While this is a crude approach to the problem it allows us to calculate in a simple fashion. Experience has shown that the rotational asymmetries introduced by this procedure are reduced by the variational trick we use.

We diagonalize, at the first step, a distorted Hamiltonian H_ε of the form

$$H_\varepsilon = H_p + \varepsilon \sum_{\vec{j}} Q^M_{\vec{j}} \tag{3.45}$$

where H_p is given by (3.6) restricted to a block of $3 \times 3 \times 3$ sites. (In performing a three-dimensional calculation we expect a priori that it will suffice to add a sum over single-site operators to distort the states, in contrast to the term used in (3.33) for the one-dimensional problem.) In subsequent steps the original Hamiltonian is truncated to the lowest six states per block. Keeping six states per site and blocking together three sites at a time requires diagonalizing a 126×126 matrix at each step (acting on the even-parity combinations of the 6^3 possible states). The variational ground-state energy density is again minimized for $\varepsilon \neq 0$.

This calculation provides a good example of the way the variational trick reduces asymmetries introduced by the blocking procedure. For $\varepsilon = 0$ the effects of the asymmetric blocking are very evident: in particular the gap to the lowest excited state is very unstable as we iterate. However as we reach the value of ε which minimizes the ground state energy density these effects are reduced: the asymmetry (in SU(4) space) introduced in the wave function by the additional term in H_ε dominates over the asymmetry introduced by the next-nearest-neighbor

terms and the gap to the lowest excited state stabilizes. We remark that these excited states probably represent massive particles; their interpretation is discussed in Section 4. The existence of a Goldstone mode is argued as before: The charge Q_5 (3.7) which commutes with (3.6) does not commute with (3.45) and hence generates a rotation of the ε term.

The approximate ground state for H formed by using the rotated H_ε^θ is degenerate with the one from the original H_ε and is orthogonal to it in the infinite volume limit. Thus, as expected, the confining flavorless theory seems to produce the physics of an Abelian σ-model with a massive vector meson.

D. Summary

We began by demonstrating the existence of θ-vacua and Goldstone bosons in the nearest-neighbor theory. We hypothesized that these phenomena would persist as non-nearest-neighbor couplings were added to break the SU(4) symmetry; an explicit calculation showed this to be true.

A check on our asymmetric blocking procedure is its application to the nearest-neighbor model. In this case it is found that for small ε the energy density does not depend on ε. We may interpret this result by noting that the SU(4) symmetric calculation had no trouble constructing the degenerate "Q vacua" for us. Thus introduction of the asymmetry served merely to combine the Q vacua into a θ vacuum. As ε grows the energy eventually goes up, as expected for a large distortion of the trial state.

4. Renormalization and Particle Masses

A. Dynamical Mass Generation

In addition to the observation of the massless particles related to the chiral symmetry breaking a further feature of these calculations is worth remarking. Although in the nearest-neighbor approximation we find only massless particles, the calculations which retain the longer-range interactions show that there are also states with a finite splitting from the ground state. For example a rotationally symmetric treatment of the 3+1 dimensional problem would give a triplet of states which transform into each other under 90^{o} rotations, split from the ground state by an amount proportional to $1/g^2a$. It is attractive to interpret this as a finite-mass spin-one meson. In order to do so we must define a renormalization scheme so that the bare quantity g^2 can be given a continuum interpretation. The proper definition of such a scheme requires calculations which we have not done. In this section we describe a reasonable scheme which we believe would emerge from a careful block-spin treatment of QCD on a lattice, and then discuss the scenario it suggests for the origins of many interesting aspects of hadron physics.

Let us start by considering the Hamiltonian (3.3) for a scale a_0 which is small enough that the relevant coupling g_0 can be chosen small: indeed so small that we can establish the correspondence of this theory with the short distance weak-coupling continuum theory. One can interpret the lattice Hamiltonian as an effective Hamiltonian which describes continuum physics with a spatial resolution greater than a_0. Were we to solve this Hamiltonian on a block of sites (say a cube of 3^3 sites), we could then write a new effective Hamiltonian by evaluating H between

wave functions spanned by the lowest few states within each block, as in the calculations just described. The new Hamiltonian can be viewed as an effective lattice Hamiltonian on a lattice with spacing $3a_0$. We define the new coefficient of the operator which measures the flux leaving a block through some face as the new effective coupling. By repeating this truncation process a number of times we would obtain a series of effective Hamiltonians $H_n(3^n a_0 , g_n)$. On the basis of the calculations[2] relating coupling strength to lattice size for a theory such as (3.3) we expect that the values of g_n and a_n so obtained would lie on a curve such as that shown in Fig. 8. The general shape of this curve must be correct, since for small $\underline{g}$ weak-coupling perturbation theory tells us to expect that the coupling grows logarithmically with increasing separation, whereas strong-coupling perturbation theory informs us that once g_n has become large then it increases linearly with increasing $\underline{a}$. The relatively sharp transition of logarithmic to linear growth shown in Fig. 8 is indicated by the calculations of Kogut *et al.*, and of Creutz. The shape of the curve is an intrinsic property of the theory which is independent of the assumed initial coupling g_0. Let us denote the distance scale at which the sharp turnover occurs as r_H and the value of g_n at that scale as g_H. Since for small g_0 the change in g_n with each iteration is small, the number $\underline{m}$ of iterations that it takes for g_m to reach g_H is clearly dependent on the starting value g_0. Thus we can write a lattice renormalization group equation of the form

$$r_H = 3^{m(g_0)} a_0 \tag{4.1}$$

The function $m(g_0)$ would be defined by carrying out the iteration calculation.

The scale r_H is the physically meaningful scale in this theory. Flux excitations of size small compared to r_H are quite probable, but flux excitations on a scale larger than r_H are highly excited states and therefore not very probable. Hence, r_H is (crudely speaking) a typical hadronic radius. To define r_H more precisely one should calculate physically measurable quantities in terms of r_H. However, this discussion makes it clear that the dimensional parameter a_0 should be defined in terms of the physically meaningful scale r_H (rather than vice versa) and that (4.1) then allows us to take a continuum limit $g_0 \to 0$, $a_0 \to 0$ with r_H held fixed.

To relate this discussion to the more familiar renormalization group discussion in perturbative continuum QCD we remark that the scale r_H corresponds to the parameter Λ which defines the intrinsic scale of QCD whereas a_0 corresponds to the physically meaningless renormalization scale μ. Thus (4.1) is similar to the first order perturbation theory equation

$$\Lambda = \mu e^{-b/g^2(\mu)} \tag{4.2}$$

Once having defined a renormalization procedure which holds r_H fixed we can then also give an interpretation to the splitting proportional to $1/g^2a$ which appears in our strong coupling calculation. This quantity can be rewritten as

$$\frac{1}{r_H} f(g_H) \tag{4.3}$$

where the function $\underline{f}$ could also be defined by an iteration calculation. In fact, all dimensionful quantities appearing in this theory would take the form (4.3), differing only in the form of the function $\underline{f}$

and the power of r_H. Once the scale r_H is defined by the calculation of some physical quantity, such as the mass of the spin one meson, then all further dimensionful quantities are calculable. The particle masses which appear in such a theory with zero quark masses are known as dynamically generated masses. The addition of small quark masses to the theory would slightly alter the particle masses from those obtained in the massless quark case.

B. Comments and Speculations

It is apparent that the ground state which our calculation constructs is highly occupied, containing many $\bar{q}q$ pairs. We remark that this is principally a matter of notation, as we are working in a chiral basis (γ_5 is diagonal) and in this basis the vacuum of the free fermion theory likewise contains many $\bar{q}q$ pairs. Were we to change basis to the more familiar (γ_0 diagonal) notation we would see that this state is just the filled Fermi sea of negative-energy states. The significant difference between the massless free fermion case and the QCD case is the nature of the long-range fluctuations which occur. In the massless free fermion theory, fluctuations in which fermion quantum numbers separate over large distances occur easily. In the QCD scenario just described, on the other hand, fermion color separation to distances large compared to r_H costs a large energy (proportional to g_H^2/r_H) and hence these fluctuations are very unlikely. Our calculations have indicated that they are replaced by coherent fluctuations (density waves) in which $q\bar{q}$ pairs move between sites, and that these are the massless (Goldstone) particles of the theory.

There are further properties of hadrons which seem to have a natural explanation within this picture:

(i) From the point of view of these calculations the effective hadronic Hamiltonian contains no coupling constant; the factor of $1/g_H^2$ appears only as an overall scale factor. Hence, the relative scale of the "kinetic terms" (those parts of H_{eff} which give rise to momentum band structure) and the remaining "quark interchange" terms (which give rise to interactions among hadrons) is of order unity. Hence the natural strength of the strong interactions is one, independent of g_H.

(ii) For 3 flavors of quarks, arguments analogous to those presented for the single-flavor theory tell us that H_{eff} will exhibit an approximate $SU(6) \otimes SU(6)$ symmetry. This symmetry differs in a crucial way from the $SU(6) \otimes SU(6)$ symmetry analyzed by Dashen and Gell-Mann[25] as a relativistic generalization of non-relativistic SU(6) first introduced by Beg and Pais.[26] This difference will be discussed in a forthcoming paper, where we will show that we are able to obtain good SU(6) predictions such as $\mu_n/\mu_p = -2/3$, but not bad ones such as $g_A/g_V \simeq 5/3$. Moreover, since PCAC appears naturally in the context of our analysis g_A/g_V will be obtained from the Adler-Weisberger relation, which is known to hold quite well. In addition we find that the sum rules for vector meson masses as well as for pseudoscalar masses appear in terms of the squares of the masses. The same discussion will show that a version of $SU(6)_W$ is a better spectroscopic symmetry for hadrons than static SU(6).

The essential ingredients in this analysis parallel the detailed discussion already given. One first divides the effective Hamiltonian

into two pieces, $H_{eff} = H_0 + V$, where H_0 contains all terms connecting sites separated by an odd number of links and V contains the remaining terms. In general, H_0 possesses an exact SU(4 × (# of quark flavors)) symmetry, which is SU(12) for the case of 3 quark flavors. Generalizing the results of our single-flavor discussion leads us to expect that the subalgebra of charges $Q_M = \sum_j \psi^+(j)\, M(j)\, \psi(j)$ -- where the M(j)'s are defined as in Eq. (3.8) -- will be realized as a symmetry of the states (i.e., in Wigner mode) for matrices M such that $[M,\gamma_0] = 0$; the remaining charges will be realized in the Goldstone mode. In the case of 3 flavors the Wigner symmetry is SU(6)⊗SU(6) and the crucial difference between it and earlier SU(6) symmetry schemes lies in the position dependence of the matrices M(j) expressed in Eq. (3.8).

(iii) We note that this picture suggests that the natural scale of gluonic excitations is of order g_H^2 in contrast to the natural scale of, say, vector meson masses which is of order $1/g_H^2$. Thus, glueball masses could be significantly different from typical hadron masses.

Finally, we must treat the U(1) problem.[27] The analysis in Section 3 has led us to a picture of the multiflavor theory wherein all axial charges, <u>including</u> the flavor-invariant U(1) charge (3.7), are associated with Goldstone bosons. It is of course desirable to eliminate the U(1) boson, and we offer a scenario within which it could "seize"[10] and disappear from the physical spectrum in the continuum limit.

If seizing were to happen it would show up in the lattice theory as follows. Consider the ordinary 1+1 dimensional Schwinger model[28] (with <u>two</u>-component fermions). Applying the same sort of perturbation theory[5] as in Section 3, one finds a glue excitation (or "photon") with mass $m_B(g_0) \sim g_0^2\Lambda$ and an effective Hamiltonian for the zero-flux gauge-

invariant states which is a version of the anisotropic SU(2) Heisenberg antiferromagnet, known to possess a massless spectrum. The scale of $H^{(2)}_{eff}$ is $\Lambda/m_B(g_0^2)$ so the boson spectrum is of the form

$$E(k) = \frac{\Lambda}{m_B(g_0^2)} k \tag{4.4}$$

where $\underline{k}$ is the momentum. It is possible to show that for fixed large Λ,

$$m_B(g_0^2) \sim g_0\Lambda \tag{4.5}$$

for $g_0 \to 0$. For conventional continuum renormalization one holds m_B fixed as Λ becomes infinite; then we find that the energy-momentum relation for the Goldstone bosons, Eq. (4.4), implies that no boson states of $k/m_B \neq 0$ can have finite energy. Therefore the continuum limit of the theory which preserves the massive photon loses all but the zero-momentum mode of the Goldstone boson.[29] This is the phenomenon which is analogous to seizing.

It is possible that seizing affects some but not all of the Goldstone bosons of QCD: although the strong-coupling calculation yields Goldstone bosons for the U(1) currents as well as for the $SU(N_f)$ currents, there is no symmetry reason for their behaviors in the $g \to 0$ limit to be the same. The U(1) boson can seize independently of the $SU(N_f)$ bosons. Verification of this conjecture would require construction of the Goldstone bosons in the weak- and intermediate-coupling regimes.

This work is supported by the Department of Energy under contract DE-AC03-76SF00515.

REFERENCES

1. K. Wilson, Phys. Rev. D10, 2445 (1975); J. Kogut and L. Susskind, Phys. Rev. D11, 395 (1975).
2. M. Creutz, Phys. Rev. Lett. 43, 553 (1979); J. B. Kogut, R. B. Pearson and J. Shigemitsu, Phys. Rev. Lett. 43, 484 (1979).
3. P. Langacker and H. Pagels, Phys. Rev. D19, 2070 (1979) and references therein.
4. Y. Nambu and G. Jona-Lasinio, Phys. Rev. 122, 345 (1961); J. Goldstone, A. Salam and S. Weinberg, Phys. Rev. 127, 965 (1962).
5. S. D. Drell, M. Weinstein and S. Yankielowicz, Phys. Rev. D14, 1627 (1976).
6. S. D. Drell, M. Weinstein and S. Yankielowicz, Phys. Rev. D16, 1769 (1977).
7. S. D. Drell, B. Svetitsky and M. Weinstein, Phys. Rev. D17, 523 (1978).
8. S. D. Drell and M. Weinstein, Phys. Rev. D17, 3203 (1978).
9. This work has been reported by B. Svetitsky, Ph.D. Thesis, Princeton University, 1980.
10. J. Kogut and L. Susskind, Phys. Rev. D10, 3468 (1974); and 11, 3594 (1975).
11. S. Coleman, Comm. Math. Phys. 31, 259 (1973).
12. S. Coleman, in Laws of Hadronic Matter, A. Zichichi, ed. (Academic Press, New York, 1975); M. Weinstein, in Springer Tracts in Modern Physics, Vol. 60, G. Hohler, ed. (Springer-Verlag, New York, 1971).

13. E. H. Lieb and D. C. Mattis, Mathematical Physics in One Dimension (Academic Press, New York, 1966).

14. H. Bethe, Z. Phys. 71, 205 (1931); J. Des Cloizeaux and M. Gaudin, J. Math. Phys. 7, 1384 (1966).

15. J. M. Rabin, Stanford Linear Accelerator Center preprint SLAC-PUB-2391 (1979) [Phys. Rev. B21, (1980, in press)].

16. For the Heisenberg model this is true when the blocking is performed with an even number of sites per block. For an odd number of sites per block the energy turns out not to depend on ϵ for small ϵ, but explicit massless states are found in the truncated spectrum. This situation arises as well as in Section 3 and the reader is referred to the discussion there for an explanation.

17. As a check on the accuracy of this method relative to the more naive approach used previously, a variant of the new method was applied to the 1+1 dimensional Ising model in a transverse field. The results were much more accurate (for a given number of states retained) than any previously obtained (M. Aelion, Ph.D. Thesis, Stanford University, 1979; M. Aelion and M. Weinstein, in preparation).

18. This restricts our discussion to the $\theta_{gauge} = 0$ sector of the theory since all locally gauge-invariant states which occur in this formalism are also invariant under the topologically non-trivial gauge transformations.

19. S. Coleman, Ann. Phys. (NY) 101, 239 (1976); P. J. Steinhardt, Ph.D. Thesis, Harvard University, 1978.

20. For example, p1 is the site $j = 3p$, p2 is $j = 3p+1$, and p3 is $j = 3p+2$.

21. We find that the splitting goes to zero more slowly than m; this may be an indication, at the crude level of this calculation, of the $\sqrt{m}$ dependence predicted by current algebra.
22. A calculation has also been carried out without this restriction; the results are essentially unchanged.
23. The distortion leaves only an SU(2) subgroup of SU(4) unbroken; the sextet of single site states decomposes into three isosinglets and one isotriplet, and we choose corresponding multiplets to comprise the truncated block basis $|i_\varepsilon\rangle$.
24. This discussion is precisely correct when only a single state is kept at each step of the truncation procedure. When more states are kept one must further show that there are no vectors in common between the states constructed with two different directions for the perturbing term.
25. R. F. Dashen and M. Gell-Mann, Phys. Lett. 17, 142 (1965); ibid. 145. This group was suggested as a relativistic generalization of non-relativistic SU(6) by K. Bardakci, J. M. Cornwall, P. G. O. Freund and B. W. Lee, Phys. Rev. Lett. 14, 48 (1965).
26. A. Pais, Rev. Mod. Phys. 38, 215 (1966).
27. See, for example, S. Weinberg, Phys. Rev. D11, 3583 (1976).
28. J. Schwinger, Phys. Rev. 128, 2425 (1962); J. Lowenstein and J. Swieca, Ann. Phys. (NY) 68, 172 (1971).
29. Even assuming that strong-coupling perturbation results are applicable as $g_0 \to 0$! Since the zero-momentum mode has zero energy, its degree of freedom is a c-number and corresponds to the chiral θ parameter.

TABLE I

The 16 Dirac matrices, rendered Hermitian. A common explicit representation is shown so that commutators may be readily evaluated.

Lorentz Structure	Dirac Matrix M^{η}	Representation
S	1	1
V	$\beta = \gamma_0$	ρ_3
	$i\gamma^i$	$-\rho_2\sigma_i$
T	$\alpha_i = -i\sigma^{oi}$	$\rho_1\sigma_i$
	$\sigma_i = \frac{1}{2}\varepsilon_{ijk}\sigma^{jk}$	σ_i
A	$i\gamma_5\gamma^o$	ρ_2
	$\gamma_5\gamma^i$	$-\rho_3\sigma_i$
P	γ_5	ρ_1

TABLE II

The six neutral site states.

$\|0\rangle$	: $b_{\uparrow}\|0\rangle = \ldots = d_{\downarrow}\|0\rangle = 0$
$\|\uparrow\uparrow\rangle$	$= b^{+}_{\uparrow} d^{+}_{\uparrow} \|0\rangle$
$\|\downarrow\downarrow\rangle$	$= b^{+}_{\downarrow} d^{+}_{\downarrow} \|0\rangle$
$\|\uparrow\downarrow\rangle$	$= b^{+}_{\uparrow} d^{+}_{\downarrow} \|0\rangle$
$\|\downarrow\uparrow\rangle$	$= b^{+}_{\downarrow} d^{+}_{\uparrow} \|0\rangle$
$\|\uparrow\downarrow\uparrow\downarrow\rangle$	$= b^{+}_{\uparrow} b^{+}_{\downarrow} d^{+}_{\uparrow} d^{+}_{\downarrow} \|0\rangle$

TABLE III

Decomposition of the generators of SU(4) with respect to $SU(2) \times SU(2) \times U(1)$, where the U(1) is generated by γ_0. Matrices labelled V and A, which commute with γ_0, generate $SU(2) \times SU(2)$ according to $J_{\pm} = V \pm A$. Multiplet structure is indicated on the right in the notation $(j_+, j_-)^U$. V commutes with α_x as well.

$\rho_3 = \gamma_0$		$(0,0)^0$
$V = \begin{bmatrix} \rho_3\sigma_2 \\ \rho_3\sigma_3 \\ \sigma_1 \end{bmatrix}$	$A = \begin{bmatrix} \sigma_2 \\ \sigma_3 \\ \rho_3\sigma_1 \end{bmatrix}$	$(1,0)^0$ + $(0,1)^0$
$\rho_1 = \gamma_5$	$\rho_1\sigma_1 = \alpha_x$	$(\frac{1}{2}, \frac{1}{2})^{+1}$ + $(\frac{1}{2}, \frac{1}{2})^{-1}$
ρ_2	$\rho_1\sigma_2 = \alpha_y$	
$\rho_2\sigma_1$	$\rho_1\sigma_3 = \alpha_z$	
$\rho_2\sigma_2$	$\rho_2\sigma_3$	

TABLE IV

Same as Table III, but where the U(1) is generated by α_x. V commutes with γ_0 as well as with α_x.

	$\rho_1\sigma_1 = \alpha_x$	$(0,0)^o$
$V = \begin{bmatrix} \rho_3\sigma_2 \\ \rho_3\sigma_3 \\ \sigma_1 \end{bmatrix}$	$A' = \begin{bmatrix} \rho_2\sigma_3 \\ -\rho_2\sigma_2 \\ \rho_1 = \gamma_5 \end{bmatrix}$	$(1,0)^o$ + $(0,1)^o$
ρ_2	$\rho_1\sigma_2 = \alpha_y$	$(\frac{1}{2}, \frac{1}{2})^{+1}$ + $(\frac{1}{2}, \frac{1}{2})^{-1}$
$\rho_3 = \gamma_0$	$\rho_1\sigma_3 = \alpha_z$	
σ_2	$\rho_2\sigma_1$	
σ_3	$\rho_3\sigma_1$	

FIGURE CAPTIONS

1. How the fermionic term in H (a) shifts the energy of the empty lattice $|0\rangle$, (b) moves a "mesonic" configuration, and (c) mixes $|0\rangle$ with a "meson," via a typical intermediate state containing two flux links.
2. Dividing the lattice into blocks of three sites each. H_p acts entirely within a block while $H_{p,p+1}$ connects two adjacent blocks.
3. Young diagrams showing the representations which arise in (a) combining two sites and (b) combining those two with a third. Dimensionality is indicated above each diagram, the value of the quadratic Casimir operator below.
4. Schematic picture of how a block-spin transformation is constructed in two dimensions, one direction at a time.
5. A manifestly x-y symmetric blocking scheme in two dimensions first couples together the sites within the dotted line and then couples in the corner sites.
6. Young diagrams for the coupling scheme which arises in the truncation depicted in Fig. 5: (a) constructing the representation on the five central sites, and (b) coupling it to the corners.
7. Young diagrams for the three-dimensional block-spin transformation: (a) coupling the face centers of the cube to the body center, (b) coupling the result to the edge centers, and (c) coupling in the corners.
8. Expected behavior of gauge coupling (coefficient of E^2) as a function of lattice size [taken from Kogut et al., Ref. 2].

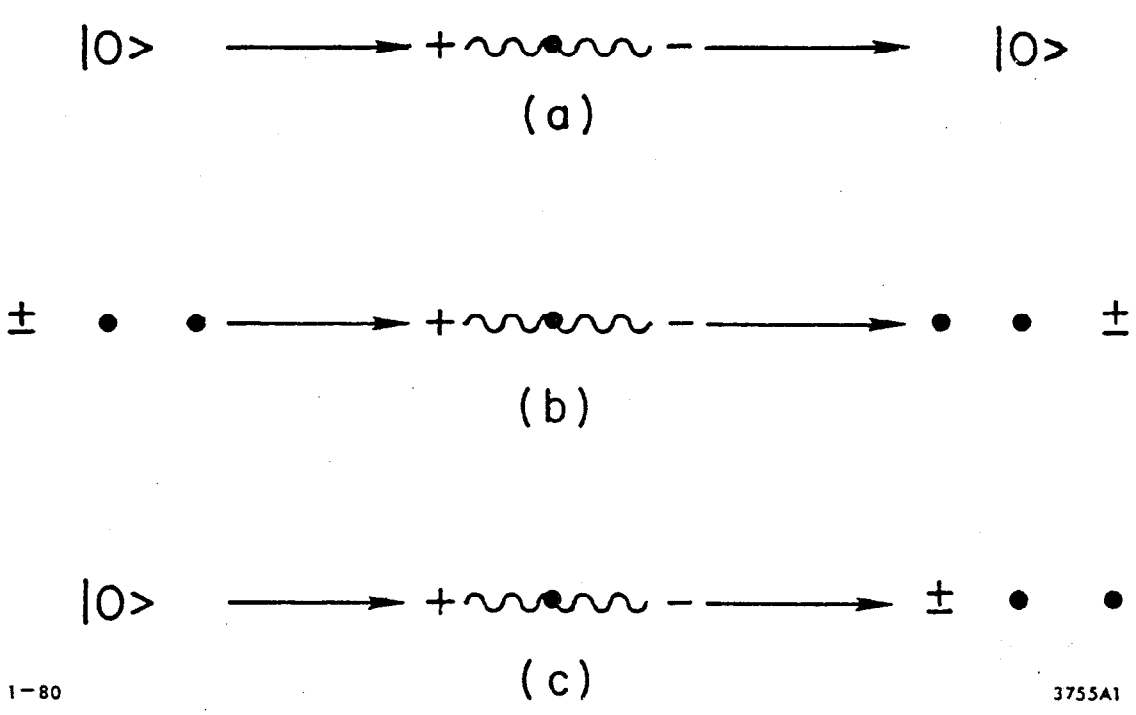

Fig. 1

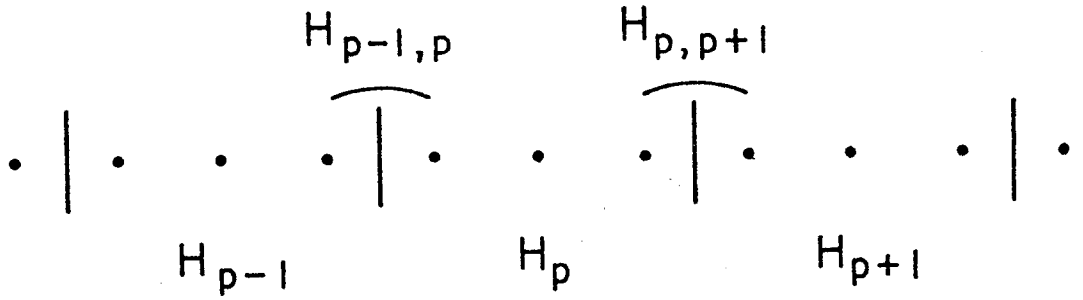

1-80

3755A2

Fig. 2

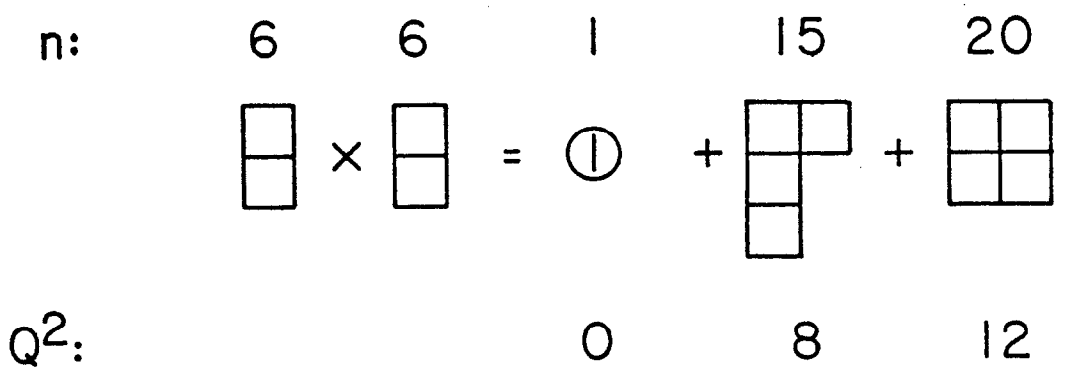

(a)

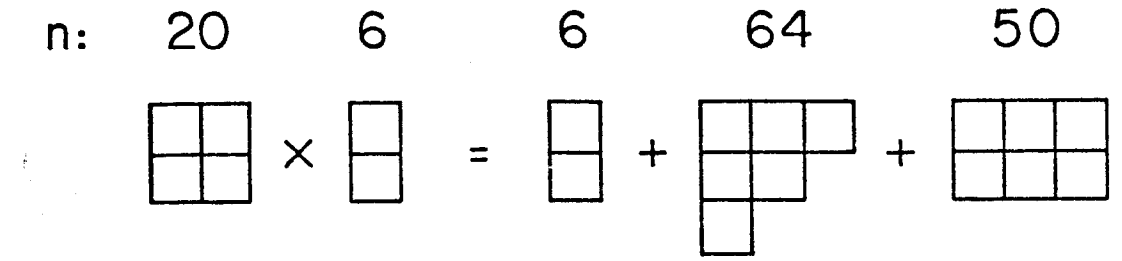

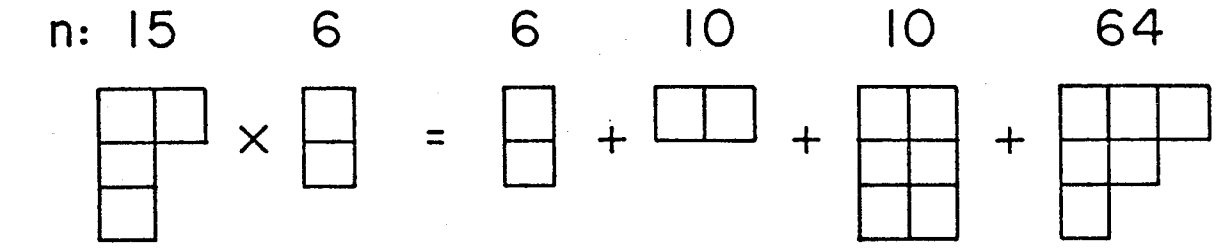

(b)

1-80

3755A3

Fig. 3

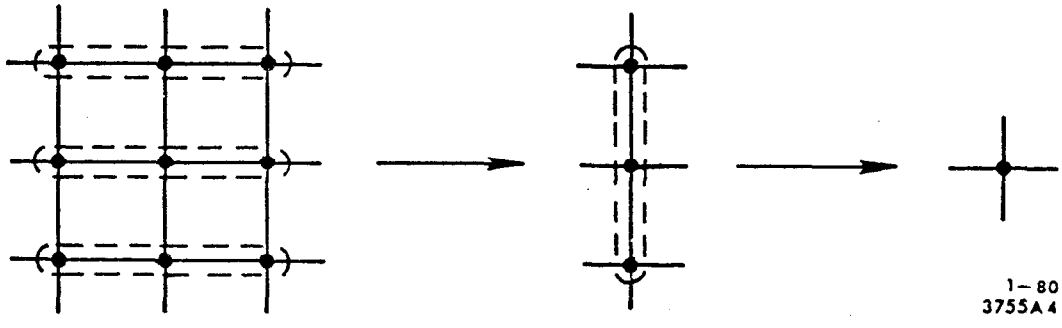

Fig. 4

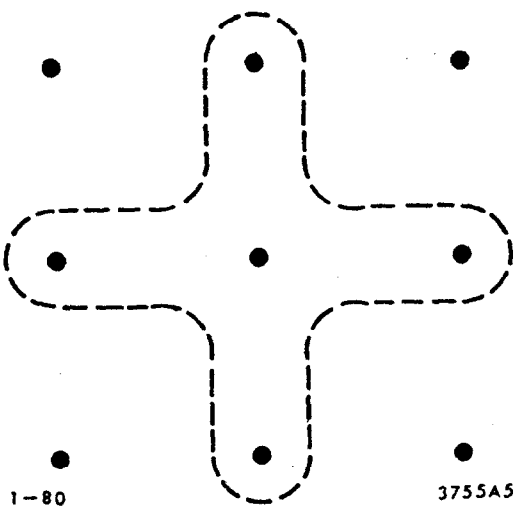

Fig. 5

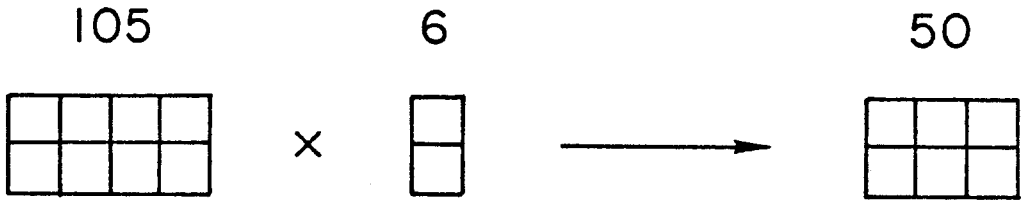

(a)

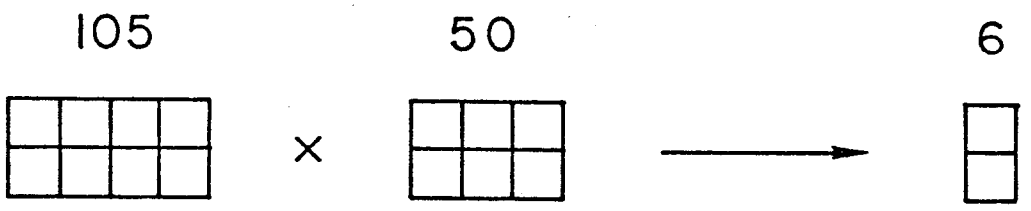

(b)

1-80

3755A6

Fig. 6

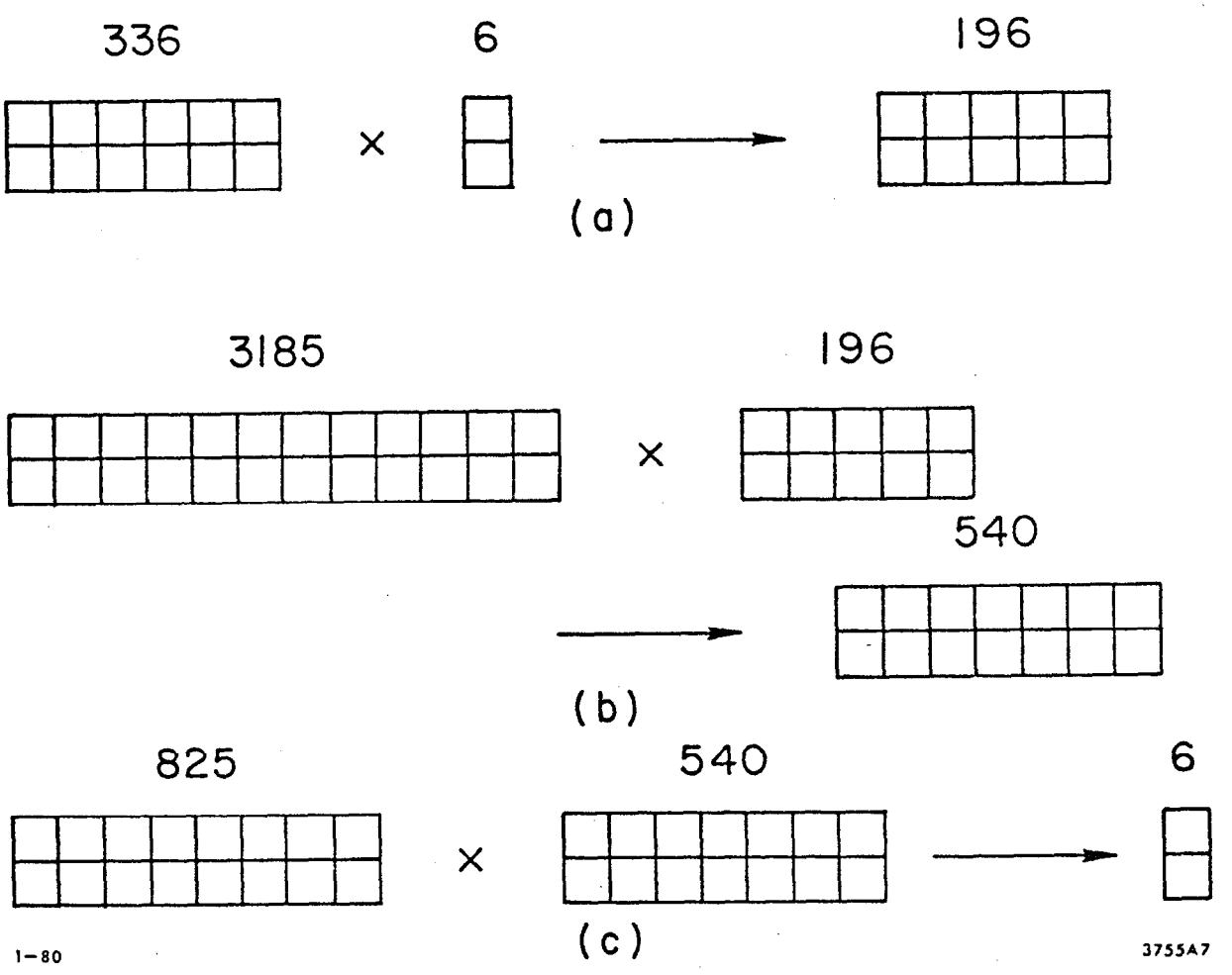

Fig. 7

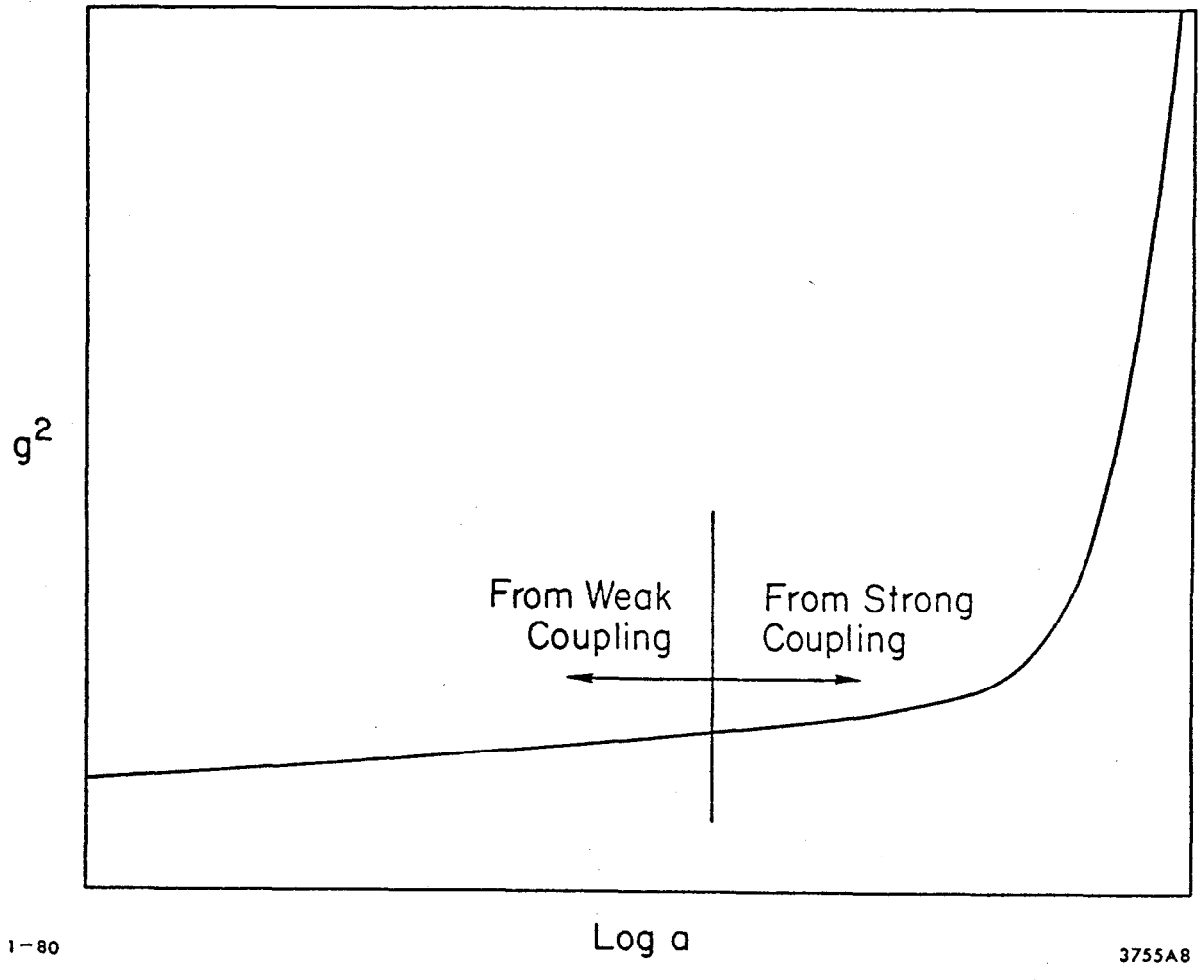

Fig. 8